PIBB 生物化学与生物物理进展
Progress in Biochemistry and Biophysics
2010, 37(4): 389~396
www.pibb.ac.cn

Temporal and Spatial Patterns of Retinal Ganglion Cells in Response to Natural Stimuli*

ZHANG Ying-Ying, JIN Xin, GONG Hai-Qing, LIANG Pei-Ji**
(*School of Life Sciences and Biotechnology, Shanghai Jiao Tong University, Shanghai* 200240, China)

Abstract Theoretical and computational studies have suggested that the visual cortex processes natural sensory information with characterized pattern that is termed as "sparse coding", which means that each individual neuron rarely fires intensely (lifetime sparseness), and meanwhile, only a small subset of neurons within a large population are activated in response to a given instantaneous stimulus (population sparseness). Temporal and spatial patterns of the chicken retinal ganglion cells′(RGCs) activities in response to time-varying natural images (movies) as well as pseudorandom white-noise checker-board flickering sequence (control) were analyzed. The sparseness indices of the RGCs′ response over lifetime and across population were calculated, the detailed temporal and spatial characteristics underlying such sparseness were also investigated. The results show that the lifetime sparseness and the population sparseness were both more profound for the neuronal responses evoked by natural stimuli as compared to that elicited by checker-board flickering. Further analysis shows that there were more action potentials fired in "burst" form in response to natural stimuli. Coincident bursts of adjacent neurons were prevalent in response to both kinds of stimulation, but occurred more frequently during natural movies stimulation. These results suggest that the RGCs encode natural sensory inputs efficiently. In this scheme, individual neuron fires at a low rate to save metabolic energy, while dynamically grouped small subsets of neurons are activated with adjacent neurons firing concertedly to transmit information to the postsynaptic neurons efficiently.

Key words lifetime sparseness, population sparseness, kurtosis, coincident bursts
DOI: 10.3724/SP.J.1206.2009.00617

During the past decades, our knowledge about visual neural information processing has been built up essentially based on experiments using simple laboratory stimuli, such as spots, bars or drifting sinusoidal gratings[1]. However, the task of the visual neural system is primarily to process information in natural environment[2]. According to some theoretical analyses, it is suggested that the visual system can use a strategy of "sparse coding" to optimize itself to match the natural scenes which are inherently "sparse" in statistical structure[3–5]. In addition to analytical results obtained from computational and theoretical studies, there are also lines of evidence provided by physiological experiments demonstrating that "sparse representations" are common in the central visual system[6–8]. In a sparse representation, various patterns of natural stimuli are encoded by concerted firings of dynamically grouped small subsets of activated neurons, such phenomenon is termed as "population sparseness"[9–10]. However, sparseness can also be defined in terms of each single neuron′s firing activity over time. In a natural environment, a single neuron is most of the time quiet or fires at a low rate, thus the terminology "lifetime sparseness" is given[10]. It has been proposed that high sparseness of the neurons′ activities in the brain should bear at least two advantages: lowering neurons′ metabolic cost by minimizing the number of active neurons at any moment[9] and improving coding efficiency with dynamically activated neuronal subsets[8].

In the present study, the activities of retinal ganglion cell (RGC) groups in response to digitized time-varying natural images (video movies) were

*This work was supported by grants from National Basic Research Program of China (2005CB724301), The National Natural Science Foundation of China (30670519) and Ministry of Education (20040248062).
**Corresponding author.
Tel: 86-21-34204015, E-mail: pjliang@sjtu.edu.cn
Received: November 12, 2009 Accepted: December 22, 2009

recorded simultaneously from isolated chicken retinas using a multi-electrode array (MEA). Pseudorandom white-noise checker-board flickering sequence was applied for control experiments. Statistical analyses performed on our experimental data demonstrate that sparseness is more remarkable for neuronal activities in response to natural stimuli as compared to that elicited by pseudorandom checker-board flickering, in a sense that both indices, lifetime sparseness and population sparseness, produce higher values for the movie-responses. To reveal the specific temporal and spatial characteristics of the neuronal activities underlying the "lifetime sparseness" and "population sparseness", we further identified the firing activities in "burst" form (densely fired action potentials) in each neuron′s spike train, and analyzed the coincident bursts across adjacent neurons. The results show that although the neurons rarely fire at high rate, adjacent neurons tend to fire "bursts" in coincidence, and this occurred more frequently during the movie-responses as compared to the checker-board-responses.

Overall, these results suggest that the RGCs′ activities are with profound metabolic economy and high coding efficiency in response to natural stimuli, thus are optimized to encode the natural stimuli which they inherently inhabit.

1 Materials and methods

1.1 Electrophysiology recording

The details of the extracellular-recording procedure have been described in our previous reports [11-12]. Briefly, retinas from chicks (about 1～3 weeks post hatching) were investigated. Action potentials fired by ganglion cells were recorded by MEA electrodes (8×8, MEA60, MCS GmbH, Germany) using a commercial multiplexed data acquisition system with a sampling rate of 20 kHz. Spikes from individual neurons were sorted using principal component analysis (PCA) [13-14], as well as the spike-detection and spike-sorting procedures provided by the commercial software MC_Rack (Multi Channel Systems MCS GmbH, Germany) and OfflineSorter (Plexon Inc. Texas, USA). Only single-neuron events consistently clarified by all these methods were adopted in further data analyses.

1.2 Visual stimulation

Stimuli were generated using programs written in VC++ and DirectX9 (unless otherwise specified), displayed on a computer monitor (796 FD Ⅱ, MAG) and projected onto the isolated retina *via* a lens system. The following stimulation protocols were applied: (1) Pseudorandom white-noise checker-board flickering sequence consisting of 1 920 frames was displayed in a 16×16 grid. The values of each sub-square of the grid were determined following an m-sequence(pseudorandom 0-1 sequence, "1" for bright and "0" for dark, with the intensities chosen as "1"= 20.01 nW/cm^2 and "0"= 0.94 nW/cm^2 to elicit the neuronal responses to a level comparable to that evoked by the natural stimuli) [15]. The checker-board frames were refreshed at a rate of 9.05 Hz, with the complete frame sequence lasted for 221 s. (2) Digitized segments of grayscale video recording of natural outdoor scenes containing trees, rocks, streets, houses etc. (download from the website of van Hateren′s lab, http://hlab.phys.rug.nl/vidlib/index.html [16]) were presented with each piece of movie containing 1 920 frames (128×128 pixels), and with a refresh rate of 10 Hz (lasted for 192 s; the mean photopic intensity was nearly 2.10 nW/cm^2).

Example frames of pseudorandom white-noise checker-board (CB) and natural movie (NM) are shown in Figure 1a and 1b. The images were of the same size while being presented on the screen and projected onto the retinal piece *via* an optical lens system. The projected images covered the whole area of the multi-electrode array.

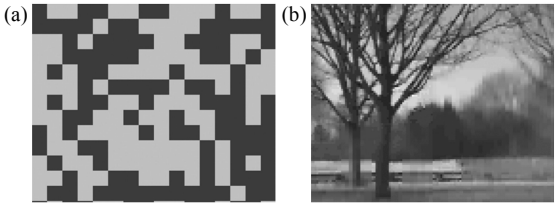

Fig. 1 Example frames

(a) Pseudorandom white-noise checker-board flickering. (b) Grayscale natural scene movie stimuli.

1.3 Sparseness measurement

Sparseness measurements were applied to characterize the firing rate distribution of individual neurons over time (lifetime sparseness) and the activity distribution of population neurons′ response at given instances (population sparseness). These two aspects of sparseness can be employed to describe the temporal and spatial characteristics of the neuronal activities. Measures of these two indices are inherently different in despite of similar computational formulae. In the present study, "kurtosis" ——the fourth moment

of a distribution, which measures its "peakedness" [10], was applied to measure the sparseness of the neuronal activities:

$$K=\left\{\frac{1}{n}\sum_{i=1}^{n}\left[\frac{r_i-\bar{r}}{\sigma_r}\right]^4\right\}-3 \quad (1)$$

For a Gaussian distribution, the K value is close to zero, while a high positive K value is related to a heavily-tailed peaky distribution.

When a neuron′s firing sequence is divided into M segments, the firing count in the ith segment can be denoted as r_i (i = 1, 2, ..., M), and the lifetime kurtosis K_L can be described as:

$$K_L=\left\{\frac{1}{M}\sum_{i=1}^{M}\left[\frac{r_i-\bar{r}}{\sigma_r}\right]^4\right\}-3 \quad (2)$$

where $\bar{r}$ and σ_r are the mean value and standard deviation of the firing counts across the M segments. A positive K_L value reflects lifetime sparseness, with larger value related to more profound sparseness.

Similar measure can be applied to assess the population sparseness. When the population contains N neurons with r_j (j = 1, 2, ..., N) being the firing count of the jth neuron in a given period, the population kurtosis K_P can be calculated as:

$$K_P=\left\{\frac{1}{N}\sum_{j=1}^{N}\left[\frac{r_j-\bar{r}}{\sigma_r}\right]^4\right\}-3 \quad (3)$$

where $\bar{r}$ and σ_r are the mean value and standard deviation of the firing counts across the N neurons during the investigated response period. Population sparseness is represented by a high positive K_P value.

In the present study, all the calculations related to sparseness assessment were performed on the binned spike trains (bin size = 200 ms) of the RGCs′ firing activities in response to the stimulation.

1.4 Coincident firing events across adjacent neurons

A group of two or more spikes with inter-spike intervals (ISIs) < 30 ms and preceded by a silent period longer than 30 ms were identified as a "burst" (as illustrated in Figure 2a). Burst identification was based on the spike times at 0.5-ms resolution. Neurons in the central visual system are sensitive to coincident input provided by their pre-synaptic neurons [17]. Thus the coincident firings might be more effective in information transmission. In the present study, the coincident firings are defined such that the firing events (including either burst or single solitary action potential) occurred between adjacent neurons (recorded from neighboring electrodes) that overlapped in time or were separated by a time interval less than 30 ms (Figure 2b). Under such a framework, we defined coincident burst events (CBB) and coincident spike events (CSS).

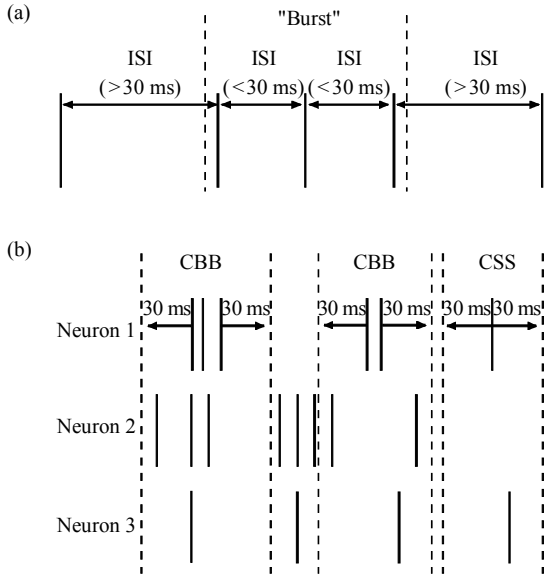

Fig. 2 Identification of burst and coincident events

(a) Sequential spikes ($n \geqslant 2$) with inter-spike intervals less than 30 ms are identified as"burst" . (b) Coincident events (CBB or CSS) are identified if the time interval between adjacent neurons' activities is less than 30 ms.

2 Results

2.1 Sparseness of the RGCs′ responses

Firing activities of an example cell (recorded from channel #36) out of the 44 neurons whose activities were simultaneously recorded from a piece of retina are plotted in Figure 3. Figure 3a and 3b are the cell′s activities in response to the 221-s CB and 192-s NM respectively (each trace represents a period of 5-s recording). The mean firing rates were 4.11 Hz and 4.17 Hz in response to CB and NM respectively. It is clearly shown that the neuron was kept silent or fired with very low rate most of the time in response to both stimuli.

Responses of the population RGCs (all the 44 neurons recorded from this retina) in a short time period (duration = 200 ms) elicited by the CB and NM are plotted in Figure 3c and 3d. It is shown that 73% (32 neurons) of the recorded neurons were kept silent, while others fired at very low rate (< 15 Hz, 3 spikes within the 200-ms) during this particular period of CB

stimulation. Meanwhile, 68% (30 neurons) were kept silent, whereas only 7% (3 neurons) fired at high rate (> 25 Hz, 5 spikes within the 200-ms time period) in response to NM.

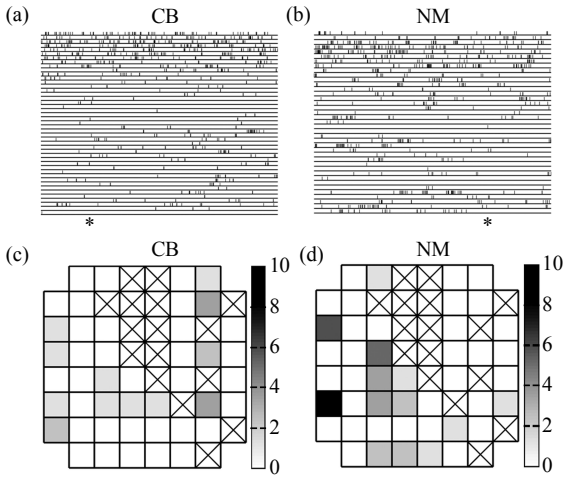

Fig. 3 Example responses of group RGCs

(a)(b) Raster plots of an example cell′s (channel #36) responses to CB and NM respectively (each vertical bar represents one spike, time bin=1 ms, each trace represents a 5-s period). The asterisks indicate the ends of the stimuli. (c)(d) Responses of the 44 RGCs during a certain segment(200 ms) of CB and NM stimulation respectively. Each grid represents the position of one electrode (60 channels available), and the firing count is represented by the grayscale (crossed grids are those failed to record any effective responses).

Response probability distributions of the example cell (channel #36) evoked by the 221-s CB and 192-s NM are plotted in Figure 4a and 4b respectively (filled bars, bin size = 200 ms). The mirror values are plotted in the negative side (blank bars) for each response probability distribution to make a comparison with a Gaussian distribution (dashed line) which shares the same mean value and standard deviation with the response probability distribution to be analyzed. The firing probability distribution of the neuronal response evoked by the CB is with a sharper peak as compared to the Gaussian distribution, with K_L = 3.780. The sparseness is more profound for the neuronal activity in response to NM, with K_L = 8.857. These results demonstrate that the null hypothesis that the firing probability distribution follows a Gaussian distribution can be rejected for the neuronal responses elicited by both CB and NM in this neuron. Distributions of firing counts of the neuron group (44 cells) during a 200-ms segment (same segment as in Figure 3c and 3d) in response to CB and NM are shown in Figure 4c and 4d respectively (filled bars). The mirror values are plotted in the negative side (blank bars) for each response distribution to make a comparison with a Gaussian distribution (dashed line) which shares the same mean value and standard deviation with the response distribution to be analyzed. When the CB was applied, the response distribution of the group neurons′ activities was with K_P=3.500. The response distribution was more peaky in exposure to NM (K_P= 10.25).

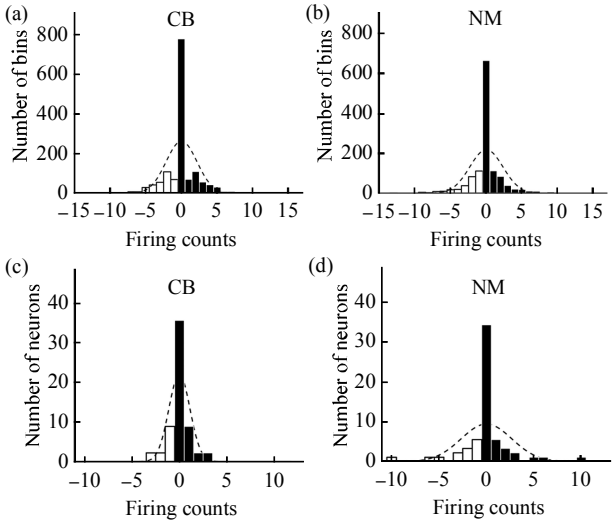

Fig. 4 The response probability distribution

(a) (b) The distributions of the neuronal activity (#36) in response to CB and NM are represented by the filled bars (the mirror values are plotted in the negative side using the hollow bars). The dashed lines represent the Gaussian distributions which shares the same mean value and standard deviation with the response distribution. (c) (d) Distributions (filled bars) of the 44 neurons′ activities in response to the 200-ms CB and NM segments. The dashed lines reflect the Gaussian distributions which share the same mean value and standard deviation as the symmetric distributions.

Figure 5a gives the statistical results of all the 44 neurons′ K_L values in response to NM against that in response to CB and Figure 5b shows the statistical results of the neuron group′s K_P values during every 200-ms segment of the NM compared with that of CB. These results reveal that the group neurons represent both the CB and NM in a sparse way, but the degree of the lifetime sparseness and the population sparseness of the neurons′ activities evoked by NM is greater than that evoked by the CB, as indicated by K_L and K_P ($P < 0.05$).

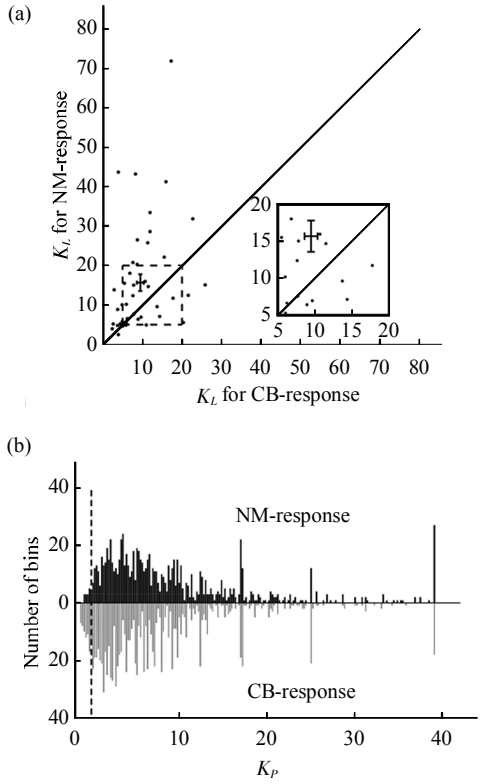

Fig. 5 Statistical results for the sparseness indices

(a) Scatter plot of the 44 RGCs′ lifetime kurtosis (K_L, time bin = 200 ms) of the NM-response against that of the CB-response. The cross error bars represent the average K_L values ($\bar{x} \pm s$) of the CB-responses and the NM-responses. Inset is truncated from the dashed box. (b) Histogram of the K_P of the group neurons′ activities in response to the 200-ms segments of the CB (black bars) and NM (gray bars).

2.2 Coincident firing activities across adjacent neurons during natural stimuli

From the neuronal firing activities plotted in Figure 3a and 3b, it is clear that although the neuron was most of the time quiet, it tended to fire action potentials in "burst" form——this happened more frequently in the cell's NM-response which can be reflected by the more remarkable lifetime sparseness of the neurons′ activities in response to NM (Figure 4b and Figure 5a). Furthermore, the long tail in Figure 4d and high population sparseness in Figure 5b also suggest that the neurons fired more frequently in coincidence in response to NM. Thus in the present study, the portion of action potentials fired in burst form (P_B) was calculated for each individual neuron, the probabilities of coincident events (coincident bursts P_{CBB} and coincident spikes P_{CSS}) occurred across adjacent neurons were also calculated.

In Figure 6a, the dots represent the P_B values for each RGCs recorded from the retina ($n = 44$) during the CB-response (horizontal axis) and NM-response (vertical axis), with the cross bars showing the mean values and the standard errors. The overall P_B values are higher for the neurons′ NM-response as compare to the neurons′ CB-response. P_{CBB} and P_{CSS} values for each RGC′s activity during CB-response (horizontal axis) and NM-response (vertical axis) are plotted in Figure 6b (the inset is truncated from the dash box), with the cross bars indicating the means and the standard errors. It is clearly demonstrated that for each individual neuron, the P_{CBB} value is higher than the P_{CSS} value, and the P_{CBB} value of NM-responses is greater than that of CB-responses in most of the neurons being investigated.

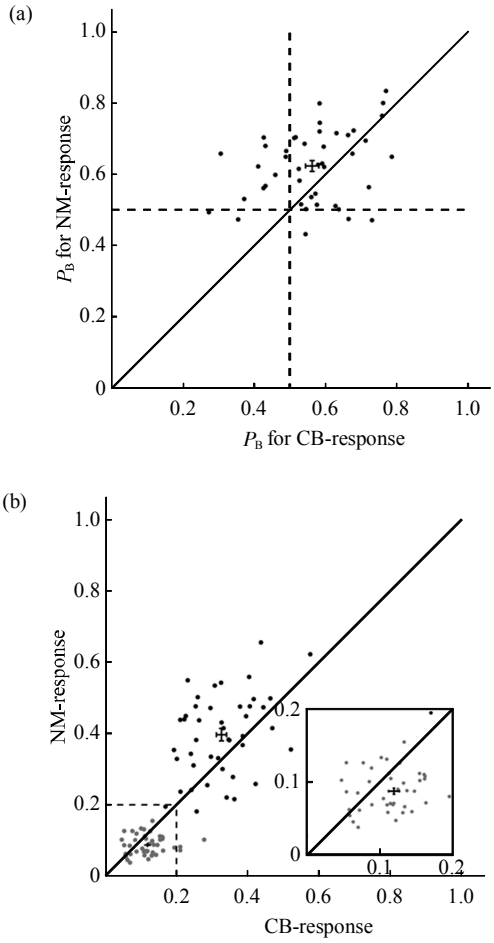

Fig. 6 Probabilities of burst patterns and coincident events

(a) P_B values of each RGC′s response during NM against that during CB. The cross bars indicate the averaged values of P_B ($\bar{x} \pm s$). (b) P_{CBB} (black dots) and P_{CSS} (gray dots) during NM-response against CB-response. Inset is truncated from the dashed box. The averaged values ($\bar{x} \pm s$) are indicated by the cross bars. •: P_{CBB}; •: P_{CSS}.

In the present study, neuronal activities were obtained from four isolated retinas (R1, R2, R3 and R4) in response to 221-s CB and three different pieces of natural movie (NM1, NM2 and NM3, each lasted for 192 s), and the analytical results are consistent across visual stimulations and retinas (data not shown). In this paper only the results of population RGCs recorded from R1 in response to CB and NM1 are presented as example. These results clearly show that the RGCs′ activities in response to NM were more frequently in burst patterns and such burst patterns were more likely to occur coincidently among adjacent neurons. It is the bursts and the coincident bursts that cause the longer tails of the individual neuron′s response probability distribution and the distribution of the population neurons′ instantaneous activities during NM, which contribute to the high lifetime sparseness and the population sparseness of the NM-responses.

3 Discussion

3.1 Physiological basis for sparse coding

The structural property of the vertebrate retina is that the photoreceptors outnumber the RGCs by a factor of tens or even hundreds, so the visual signal generated by the photoreceptors is transferred to the RGCs in a convergent way before it is further projected to the central visual part in a divergent way. The optical nerve, which is formed by the axon fibers of the RGCs, can therefore be the structural bottle-neck of the whole visual system if the RGCs are independent channels for information transmission. Data from multi-electrode recordings have actually revealed that RGCs can be grouped up in a dynamic way in response to different stimuli, to ensure the information transmission[18]. This is to say that even a single RGC is involved in multiple tasks, and "busy" activities are expected for the ganglion cells to encode the visual information properly, while the visual cortical neurons are highly developed with their functions highly specified, allowing those cells have sparse representation of the natural stimuli.

Since the firing activity is energy-consuming and the dynamic range of effective firing rates is limited, it has been proposed that the early-stage neurons in visual system might also encode the natural stimulation using a strategy of "sparse coding"[19]. In primates, the visual information encoded by the RGCs is faithfully sent to the visual cortex through LGN, whilst the LGN also receives centrifugal inputs from the superior colliculus and V1 at least in some species[20]. LGN neurons resemble RGCs in receptive field and dynamic range, thus suffer from the similar "bottle-neck" problem. However, it was reported that the cat LGN neurons′ responses during both white-noise stimuli and natural visual stimuli showed the property of lifetime sparseness, the degree of which was affected by the contrast as well as the spatiotemporal correlation of the stimulus[6]. So the "bottle-neck" structure of the LGN layers does not necessarily require the LGN neurons be always busy. Instead, the population neurons may extend their encoding capacity by firing in dynamic groups, which leads to the sparse representation of the LGN neurons. This was also the case for the RGCs investigated in our present work.

3.2 Properties of the stimuli and the response

The sparseness of the neuronal activities might be related to several aspects of stimuli properties and the adaptation strategy of the RGCs in dealing with the visual stimulation. Intuitively, the spatial and temporal properties of the stimuli should be determinant to the spatial and temporal properties of RGC activities. The contrast of the natural stimuli in a particular part of the visual field is most of time changing continuously with only a few sudden and sharp changes, in spite of the large intensity variation of the natural image streams. Such temporal and spatial properties of the natural stimuli often result in intermittent adaptation of individual RGC′s response activity over lifetime and make the population neurons grouping up dynamically to fire coincident spikes during the stimuli. However the lifetime sparseness of the CB-responses was more likely to be resulted from the overall adaptation in response to continuous pseudo-random white-noise checker-board flickering.

3.3 Temporal and spatial patterns underlying sparseness and physiological significance

As illustrated in Figure 4, it is clear that the high value of kurtosis (sparseness) is related to two aspects of the response distribution, one is the high probability at/near zero, the other is the long tail of the distribution, which means that although the neurons are most of time quiet or fire at low rates, they actually may fire at high rates and fire coincidently at certain instants. We therefore took a further step to look into the detailed response structure underlying the sparseness.

Physiologically, it is believed that the

postsynaptic neurons′ spikes are inherited from the presynaptic neurons′ spikes, i.e., an EPSP is necessary (although not sufficient) for producing a spike in the postsynaptic neuron. Several studies showed that a single RGC′s sequential spikes with ISI less than 30 ms facilitated the postsynaptic LGN neuron′s firing activity [21-22]; coincident spikes of the nearby input neurons enhanced the firing probability of the target visual cortical neurons [17]. Therefore, in the present study, the burst pattern was defined as sequential spikes with ISI shorter than 30 ms and the coincident firing events were characterized as firing activities of adjacent neurons with time difference shorter than 30 ms.

The results show that the single RGCs′ activities during natural stimuli occurred more frequently in burst patterns, which was suggested to be more efficient to evoke the postsynaptic neurons [22]; furthermore, the burst activities were more often coincident with adjacent neurons′ firing events, which could also facilitate the target neuron′ activities if the neurons project to the same post-synaptic neurons.

Acknowledgements The authors thank Dr X-D Jiang and Mr B Li for their contributions to stimulation program writing.

References

[1] Rust N C, Movshon J A. In praise of artifice. Nat Neurosci, 2005, **8**(12): 1647-1650

[2] Reinagel P. How do visual neurons respond in the real world?. Curr Opin Neurobiol, 2001, **11**(4): 437-442

[3] Dong D W, Atick J J. Statistics of natural time-varying images. Network: Comput Neural Syst, 1995, **6**: 345-358

[4] Field D J. Relations between the statistics of natural images and the response properties of cortical cells. J Opt Soc Am A, 1987, **4**(12): 2379-2394

[5] Olshausen B A, Field D J. Vision and the coding of natural images. American Scientist, 2000, **88**: 238-245

[6] Lesica N A, Jin J, Weng C, *et al*. Adaptation to stimulus contrast and correlations during natural visual stimulation. Neuron, 2007, **55** (3): 479-491

[7] Vinje W E, Gallant J L. Sparse coding and decorrelation in primary visual cortex during natural vision. Science, 2000, **287** (5456): 1273-1276

[8] Weliky M, Fiser J, Hunt R H, *et al*. Coding of natural scenes in primary visual cortex. Neuron, 2003, **37**(4): 703-718

[9] Field D J. What is the goal of sensory coding?. Neural Computation, 1994, **6**: 559-601

[10] Willmore B, Tolhurst D J. Characterizing the sparseness of neural codes. Network, 2001, **12**(3): 255-270

[11] Liu X, Zhou Y, Gong H Q, *et al*. Contribution of the GABAergic pathway(s) to the correlated activities of chicken retinal ganglion cells. Brain Res, 2007, **1177**: 37-46

[12] Chen A H, Zhou Y, Gong H Q, *et al*. Luminance adaptation increased the contrast sensitivity of retinal ganglion cells. Neuro Report, 2005, **16**(4): 371-375

[13] Zhang P M, Wu J Y, Zhou Y, *et al*. Spike sorting based on automatic template reconstruction with a partial solution to the overlapping problem. J Neurosci Methods, 2004, **135**(1-2): 55-65

[14] Wang G L, Zhou Y, Chen A H, *et al*. A robust method for spike sorting with automatic overlap decomposition. IEEE Trans Biomed Eng, 2006, **5**(6): 1195-1198

[15] Lesica N A, Stanley G B. Encoding of natural scene movies by tonic and burst spikes in the lateral geniculate nucleus. J Neurosci, 2004, **24**(47): 10731-10740

[16] van Hateren J H, van der Schaaf A. Independent component filters of natural images compared with simple cells in primary visual cortex. Proc Biol Sci, 1998, **265**(1394): 359-366

[17] Usrey W M, Alonso J M, Reid R C. Synaptic interactions between thalamic inputs to simple cells in cat visual cortex. J Neurosci, 2000, **20**(14): 5461-5467

[18] Meister M, Berry M J. The neural code of the retina. Neuron, 1999, **22**(3): 435-450

[19] Olshausen B A, Field D J. Sparse coding of sensory inputs. Curr Opin Neurobiol, 2004, **14**(4): 481-487

[20] Briggs F, Usrey W M. A fast, reciprocal pathway between the lateral geniculate nucleus and visual cortex in the macaque monkey. J Neurosci, 2007, **27**(20): 5431-5436

[21] Usrey W M, Reppas J B, Reid R C. Paired-spike interactions and synaptic efficacy of retinal inputs to the thalamus. Nature, 1998, **395**(6700): 384-387

[22] Sincich L C, Adams D L, Economides J R, *et al*. Transmission of spike trains at the retinogeniculate synapse. J Neurosci, 2007, **27**(10): 2683-2692

视网膜神经节细胞对自然刺激的时空反应模式*

张莹莹 金 鑫 龚海庆 梁培基**
(上海交通大学生命科学技术学院，上海 200240)

摘要 神经系统信息处理的理论研究和计算结果表明，视皮层可以通过稀疏编码 (sparse coding) 模式来处理自然刺激信息. 神经元群体中，单个神经元在大多数时间里没有强的脉冲发放 (时间维稀疏性，lifetime sparseness)，而针对某一刺激，只有少数神经元在特定的时间内发放 (空间维稀疏性，population sparseness). 从神经元放电的时间和空间模式两个方面考察了视网膜神经节细胞群体对自然刺激(电影)的编码方式，并同实验室常用的伪随机棋盘格刺激下视网膜的反应模式进行比较，分析了视网膜神经节细胞反应的稀疏性指标，并深入探讨了其内在的时间和空间特点. 结果提示，视觉系统在其最初阶段——视网膜——即开始采用一种高效节能的稀疏编码方式来处理自然视觉信息，单个神经元的时间维稀疏性节省了代谢能量消耗，而群体神经元中邻近神经元的动态成组协同发放，提高了信息向突触后神经元传递的有效性.

关键词 时间维稀疏性，空间维稀疏性，峰度，同步脉冲串
学科分类号 Q42 **DOI:** 10.3724/SP.J.1206.2009.00617

* 国家重点基础研究发展计划(973)(2005CB724301), 国家自然科学基金(30670519)和教育部(20040248062)资助项目.
** 通讯联系人.
Tel: 021-34204015, E-mail: pjliang@sjtu.edu.cn
收稿日期：2009-11-12，接受日期：2009-12-22